Journal of Thermal Analysis and Calorimetry, Vol. 87 (2007) 3, 747–751

SYNTHESIS AND CHARACTERIZATION OF $Pb_{1-x}La_xTiO_3$ NANOCRYSTALLINE POWDERS

A. Mesquita, M. I. B. Bernardi, L. J. Q. Maia and V. R. Mastelaro*

Instituto de Física de São Carlos, Universidade de São Paulo, São Carlos, SP, Brazil

$Pb_{1-x}La_xTiO_3$ (PLT) nanocrystalline powders were obtained by polymeric precursor method. The samples were analyzed by differential scanning calorimetry (DSC) and thermogravimetry (TG) techniques to characterize properly the distinct thermal events occurring during synthesis. The X-ray diffraction patterns show a tetragonal structure for the samples with x=0.10 and 0.15. An increase of the lanthanum concentration to x=0.20 led to a highly symmetric structure, cubic on average. The powders obtained at the end of the synthesis had an average particle size of 30 to 70 nm.

Keywords: *nanocrystalline powders, $Pb_{1-x}La_xTiO_3$, polymeric precursors*

Introduction

Lead titanate, $PbTiO_3$ (PT), is a well known perovskite-type ferroelectric ceramic. Substitution of Pb^{2+} ions by La^{3+} ions improves the mechanical and ferroelectric characteristics of PT [1–5]. Due its potential technological applications as dynamic random access memories and infrared sensors [1–5] lead lanthanum titanate ($Pb_{1-x}La_xTiO_3$ or PLT) system has been studied extensively. Physical properties of PLT samples depend mainly on the lanthanum concentration. In those samples prepared by a solid-state reaction method a normal ferroelectric behavior was observed for $x\leq0.25$, whereas a relaxor behavior was observed when x=0.30 [6].

It is well known that grain size, morphology and crystalline structure govern the ferroelectric domain structure [7]. In particular, experimental studies have reported two critical sizes that exert major influence on ferroelectricity. The first, which occurs in the sub-micron size range is characterized by a transition from multi-domain to single-domain grains. This transition has been found to be around 200 nm in $PbTiO_3$ thin films and about 300 nm in $PbZr_{0.95}Ti_{0.05}O_3$ crystallites. The second critical grain size involves the disappearance of ferroelectric behavior. In this case experimental studies reported a critical size in the nanometric range, such as 30 nm for $BaTiO_3$ powder particles and 7–14 nm for $PbTiO_3$ thin films.

These findings indicate that the critical particle size can vary in large extent from one system to another one resulting significant changes in the ferroelectric property. Thus, it seems in it important to determine the critical grain size of different ferroelectric materials, including the $Pb_{1-x}La_xTiO_3$ system. To this end, nanocrystalline powder samples with a relatively narrow size distribution must first be produced. Several chemical methods such as sol–gel, stearic-acid gel and hydrothermal method have recently been applied to prepare PT and PLT nanocrystals. In the present study, $Pb_{1-x}La_xTiO_3$ nanocrystals with $0.10\leq x\leq0.20$ were prepared using the polymeric precursor method, also referred as the Pechini method [8]. This method enabled us to produce nanocrystalline powder samples at a relatively low temperature. Thermal and structural properties of the samples were analyzed as a function of the lanthanum content and annealing temperature using differential scanning calorimetry (DSC), thermogravimetric analysis (TG) and X-ray diffraction (XRD) techniques.

Experimental

Polymeric precursor method is based on the polymerization of metallic citrate using ethylene glycol [9]. A hydrocarboxylic acid such as citric acid is normally used to chelate cations in an aqueous solution. The addition of a polyalcohol such as ethylene glycol leads to the formation of an organic ester. Polymerization promoted by heating to around 100°C results a homogenous resin in which the metal ions are distributed uniformly throughout the organic matrix.

Lead acetate trihydrate [$(CH_3CO_2)_2Pb{\cdot}3H_2O$], lanthanum nitrate hexahydrate [$La(NO_3)_3{\cdot}6H_2O$)] and titanium(IV) isopropoxide $Ti[OCH(CH_3)_2]_4$ were used as precursors. Titanium citrate was formed by dissolution of titanium(IV) isopropoxide in a citric acid aqueous so-

* Author for correspondence: amesquita@ursa.ifsc.usp.br

1388–6150/$20.00

Akadémiai Kiadó, Budapest, Hungary
Springer, Dordrecht, The Netherlands

lution (60–70°C) under constant agitation. Lanthanum nitrate and lead acetate were dissolved in water and then were added to an aqueous acid citric solution. For x=0.15 (PLT15) and x=0.20 (PLT20) samples, ammonium hydroxide was added to the solution to adjust the pH, thereby preventing the precipitation of lead acetate until dissolution was complete. Addition of ammonium hydroxide adjusts the pH to around 4–5 in both samples. Titanium citrate was added to this second solution, after when ethylene glycol ($HOCH_2CH_2OH$) was mixed to promote polymerization of the citrate by a polyesterification reaction. 1:1 molar ratio of lead-lanthanum and titanium cations was kept. The citric acid:metal molar ratio was 3:1, while the citric acid:ethylene glycol ratio was 60:40 (mass ratio) or 3.0:6.1 (molar ratio).

The thermal decomposition and crystallization processes were studied by TG (Netzsch STA 409C) and DSC techniques under oxygen atmosphere at a heating rate of 5°C min^{-1}. Al_2O_3 was used as reference material during the thermal analysis. Before starting these measurements, the resins were dried for 15 days at 80°C, in the case of PLT10, and at 120°C in that of the PLT15 and PLT20 compositions.

After annealing at 600°C for 2 h, the powders were structurally characterized using an automatic diffractometer (Rigaku, Rotaflex RU200B) with CuK_α radiation (50 kV/100 mA, 1.5405 Å) and a graphite monochromator. The scanning range was between 10 and 70° (2θ) with a step size of 0.02° and a step time of 1.0 s. The microstructural characterization was carried out using a high resolution scanning electron microscope (FEG-SEM Supra 35, Zeiss, Germany) operating at 3 kV.

Results and discussion

Thermal analysis

Figure 1 presents the TG and DSC curves of PLT10, PLT15 and PLT20 resins. Although the method is basically semi-quantitative, the variations in masses can be correctly measured. The TG curves reveal a series of overlapped decomposition reactions due to different exothermal events, as indicated by the DSC curves. Table 1 presents the temperature range and the respective thermal event of each reaction.

The total mass loss of each composition varied from 84 to 91%. However, no mass loss was observed in the PLT10 sample above 467°C and in the PLT15 and PLT20 samples above 510°C. At these temperatures, the polymeric combustion was concluded and the residual organic materials were completely eliminated. As it can be seen, the addition of ammonium hydroxide delays the polymeric chains' pyrolysis process (oxidation and combustion), increasing their stability. In the range of 50 to 160°C, PLT10, PLT15 and PLT20 samples presented around 4.9, 4.5 and 2.8% of mass losses, respectively. These losses resulted from the elimination of H_2O and NH_3 formed during the complexation of metals and chain polymerization from isopropyl alcohol, acetic acid and NO_x.

Four thermal superposed events are visible in the TG curve of PLT10 resin: the substantial mass loss of 48.5% from 160 to 291°C is related to dehydration of the resin, which became anhydrous, and to the breakdown of weakly bonded CH_2 groups. These groups oxidized from the oxygen-rich atmosphere, forming CO/CO_2 and H_2O species. Furthermore, the CH_2 groups continued to breakdown between 291 and 347°C, leading to a mass loss of about 13.5%. The elimination of C–O groups began in the subsequent interval from 347 to 391°C, with a mass loss of 15.9%. Finally, the mass loss of 16.5% between 391 and 467°C was attributed to the elimination of strongly bonded carbon atoms (M–O–C groups).

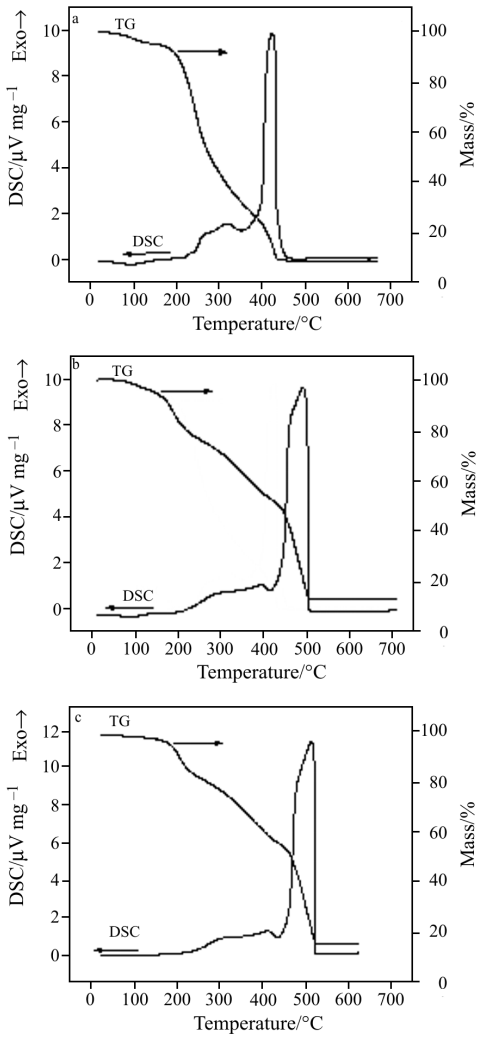

Fig. 1 DSC and TG curves of a – PLT10, b – PLT15 and c – PLT20

On the other hand, only three thermal events accompanied by mass loss took place in the PLT15 and PLT20 samples, with the largest mass loss occurring at the end of the combustion process. The PLT15 and PLT20 samples underwent a mass loss of 18 and 17% between 160 and 260°C, respectively, and of 22.8 and 25.4% between 260 and 420°C. The last decomposition event, which led to a mass loss of 38.6 and 42.5%, occurred between 420 and 510°C for PLT15 and PLT20, respectively. The reaction that occurs in this temperature range can be described as follows. It is well known that the complexation of titanium with citric acid leads to the following reaction:

$$Ti[OCH(CH_3)_2]_4+4C_6O_7H_8\rightarrow$$
$$Ti(C_6O_7H_7)_4+4(CH_3)_2CHOH \quad (1)$$

where Ti citrate and isopropyl alcohol are formed. On the case of lanthanum, its complexation leads to:

$$La(NO_3)_3\cdot 6H_2O+3C_6O_7H_8\rightarrow$$
$$La(C_6O_7H_7)_3+3HNO_3+6H_2O \quad (2)$$

forming nitric acid and water, which leads to the complexation:

$$(CH_3CO_2)_2Pb\cdot 3H_2O+2C_6O_7H_8\rightarrow$$
$$Pb(C_6O_7H_7)_2+2CH_3COOH+3H_2O \quad (3)$$

with the formation of acetic acid and water.

Mixing these metallic complexes (metallic citrates) above 70°C triggers the onset of the esterification reaction between metal citrate and ethylene glycol, as follows:

$$M^{3+}[OCOCH_2C(OH)(COOH)CH_2COOH]_3+$$
$$+3HOCH_2CH_2OH\rightarrow$$
$$M^{3+}[OCOCH_2C(OH)(COOH)CH_2COOCH_2CH_2OH]_3+$$
$$+3H_2O \quad (4)$$

In the compounds studied here, the polyesterification reactions (reaction (4)) occurred continuously until the polymeric network was formed. Based on these reactions, the following basic units can be formed in the polymeric network:

$$\{Ti^{4+}[OCOCH_2C(OCH_2–\ldots)$$
$$(COOCH_2–\ldots)CH_2COOCH_2–\ldots]_4\}$$
$$\ldots\{La^{3+}[OCOCH_2C(OCH_2–\ldots)$$
$$(COOCH_2–\ldots)CH_2COOCH_2–\ldots]_3\}x$$
$$\ldots\{Pb^{2+}[OCOCH_2C(OCH_2–\ldots)$$
$$(COOCH_2–\ldots)CH_2COOCH_2–\ldots]_2\}(1–x) \quad (5)$$

Therefore, the main organic compounds contained in the resin are alcohol, water, acetic acid, nitric acid and polyester.

Based on these results, it can be concluded that this system is highly reactive in an oxidizing atmosphere, requiring 30.5 mols of O_2 per $TiPb_{0.90}La_{0.10}C_{54.9}O_{42.7}H_{61}$ unit to achieve the above described reactions. A similar analysis can be made for the PLT15 and PLT20 samples.

With regard to the DSC curves, they are very similar. However, there is a visible displacement in the position of the peaks related to the decomposition reactions of organic compounds in the samples containing ammonium hydroxide. Each decomposition reaction observed by DSC was exothermic. Crystallization occurred immediately after the decomposition reaction. In the PLT10 sample, the crystallization peak overlapped with the peak of the last decomposition reaction. The highest crystallization peak occurred at around 427°C for the PLT10 sample and at about 491 and 499°C for the PLT15 and PLT20 samples, respectively.

Table 1 Representative thermal transitions of PLT samples

Sample	Temperature range/°C	Mass loss/% (from TG)	Mass loss/% of anhydrous polymer, calculated from reduced formula	Thermal event
PLT10	30–160	5.1	–	H_2O, NO_x, alcohol, acetic acid
	160–291	48.5	–	H_2O, NO_x, polymer degradation
	291–347	13.5	13.4	polymeric degradation (–CH_2– groups)
	347–391	15.9	29.2	polymeric degradation
	391–467	16.5		(–CO– and –COO– groups)
	above 467	–	–	9.1% of residual mass/$Pb_{0.90}La_{0.10}TiO_3$
PLT15	30–160	5.6	–	H_2O, NO_x, alcohol, acetic acid, NH_4
	160–260	17.9	–	H_2O, NO_x, NH_4, polymer degradation
	260–420	22.8	22.4	polymeric degradation (–CH_2– groups)
	420–510	38.6	48.8	polymeric degradation (–CO– and –COO– groups)
	above 510	–	–	15.1% of residual mass=$Pb_{0.85}La_{0.15}TiO_3$
PLT20	30–160	2.5	–	H_2O, NO_x, alcohol, acetic acid, NH_4
	160–260	16.9	–	H_2O, NO_x, NH_4, polymer degradation
	260–420	25.4	19.3	polymeric degradation (–CH_2– groups)
	420–510	42.5	41.9	polymeric degradation (–CO– and –COO– groups)
	above 510	–	–	12.8% of residual mass=$Pb_{0.80}La_{0.20}TiO_3$

Based on these results, it seems reasonable to assume that ammonium hydroxide facilitates the dehydration of ethylene glycol (a catalyst effect), favoring a more efficient polyesterification reaction and forming more stable polymeric clusters at high temperatures. The decomposition of PLT15 and PLT20 samples took place at higher temperature than PLT10 prepared without ammonium hydroxide.

X-ray diffraction

Figure 2a shows the X-ray diffraction patterns at room temperature for PLT samples calcined at 600°C for 2 h at a heating rate of 10°C min^{-1}. For the sake of comparison, the XRD pattern of the PLT00 sample (pure $PbTiO_3$ or PT) is also presented. Firstly, it can be observed that the samples crystallized completely without the presence of secondary phases. The XRD pattern of pure PT was indexed as presenting a tetragonal structure with a P4mm space group, which is in agreement with the literature [10]. When Pb atoms were replaced by La in the $PbTiO_3$ lattice a superposition of the reflections characteristic of tetragonal structure was observed, mainly those of the (001) and (100) and (002) and (200) diffractions planes (Fig. 2b). This superposition clearly indicates that the degree of tetragonality decreased as the amount of La increased. Thus, a transition to higher symmetric phase, in this case a cubic perovskite structure with a Pm-3m space group was observed in the PLT20 sample [11]. The overlapping of these diffraction peaks with increasing amounts of La was also observed in samples prepared by the conventional solid-state reaction method [6]. However, in that case the overlapping occurred only in samples with x>0.25 (PLT25), indicating that the reduced grain size leads to a lower degree of tetragonality (c/a) with smaller amounts of La.

Morphology

Figure 3 shows the surface microstructure of PLT nanopowders. Note that the microstructure seems to be quite strongly affected by the addition of ammonium hydroxide. PLT10 nanopowders, consisting of quasi-spherical nanoparticles, showed uniform grains with an average size of around 30±5 nm. The average grain size of PLT15 and PLT20 samples ranged from 50 to 70±5 nm and, congruous with previous results reported by other authors, exhibited a significant coalescence process [12].

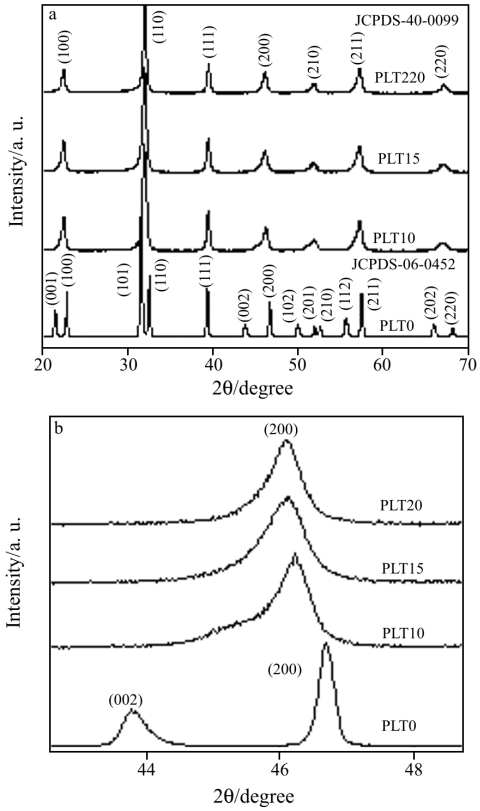

Fig. 2 XRD patterns of a – PLT10, PLT15 and PLT20 powders heat treated at 600°C for 2 h heated at a 10°C min^{-1} and b – detail between 43 and 48°

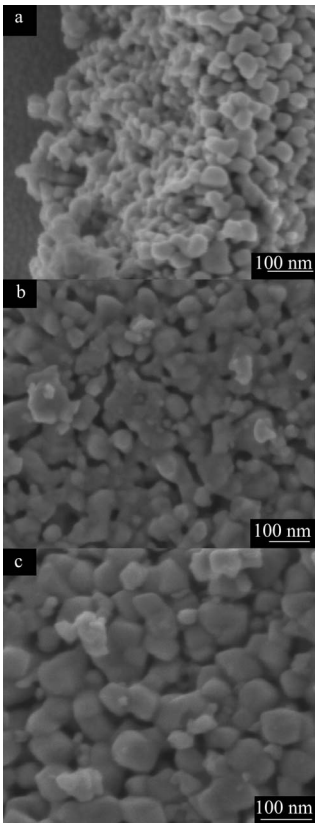

Fig. 3 SEM-FE micrographs of a – PLT10, b – PLT15 and c – PLT20 nanopowders annealed at 600°C/2 h

Conclusions

In conclusion, PLT nanopowders were obtained by the polymeric precursor method. A description was given of the reactions occurring during the synthesis of precursor solutions. The use of DSC and TG techniques allowed the description of the decomposition and crystallization processes, as well as to define the temperature range in which thermal events occur, such as pyrolysis of organic compounds, nitrate evaporation and water elimination. Increasing the lanthanum concentration caused a structural phase transition from tetragonal to 'cubic' symmetry. Nanometric particles with grain sizes ranging from 30 to 70 nm were obtained.

Acknowledgements

The authors acknowledge FAPESP, CAPES and CNPq (Brazil) for their financial support.

References

1 S. Murakami, M. Herren, D. Rau, T. Sakurai and M. Morita, J. Lumin., 83/84 (1999) 215.
2 A. K. Arora, R. P. Tandon and P. Mansingh, Ferroelectrics, 132 (1992) 9.
3 T. Utsunomiya, Jpn. J. Appl. Phys., 33 (1994) 5440.
4 A. Sternberg, Ferroelectrics, 134 (1992) 29.
5 M. Okuyama, J.-I. Asano and Y. Hamakawa, Jpn. J. Appl. Phys., 33 (1994) 5506.
6 P. P. Neves, A. C. Doriguetto, V. R. Mastelaro, L. P. Lopes,Y. P. Mascarenhas, A. Michalowicz and J. A. Eiras, J. Phys. Chem. B, 108 (2004) 14840.
7 S. Berger, Transac. Indian Inst. Metals, 58 (2005) 1141.
8 M. P. Pechini, U.S. Patent 3 330 697 (1967).
9 M. R. Cassia-Santos, A. G. Souza, L. E. B. Soledade, J. A. Varela and E. Longo, J. Therm. Anal. Cal., 79 (2005) 415.
10 O. Yamaguchi, A. Narai, T. Komatsu and K. Shimizu, J. Am. Ceram. Soc., 69, C256 (1986) – JCDPS: 40-0099.
11 Natl. Bur. Stand (US), Circ. 539, 5, 39 (1955) – JCPDS: 06-0452.
12 F. M. Pontes, J. H. Rangel, E. R. Leite, E. Longo, J. A. Varela, E. B. Araújo and J. A. Eiras, J. Mater. Sci., 36 (2001) 3565.

DOI: 10.1007/s10973-006-7760-6